Structure and Solvation in Ionic Liquids

CHRISTOPHER HARDACRE,*,†,‡
JOHN D. HOLBREY,†,‡
MARK NIEUWENHUYZEN,† AND
TRISTAN G. A. YOUNGS‡,§

School of Chemistry and Chemical Engineering, The QUILL Centre and School of Maths and Physics, Queen's University Belfast, Belfast BT9 5AG, U.K.

Received March 17, 2007

ABSTRACT

This Account describes experimental data used to understand the structure of ionic liquids and solute–solvent interactions of both molecular solutes and dissolved metal complexes. In general, the structures of the ionic liquids determined from experimental data show good agreement with both simulated structures and solid-state structures. For all ionic liquids studied, strong charge ordering is found leading to long-range order even in the presence of a solute. For dissolved metal complexes, the ionic liquid is not innocent and a clear dependence on the speciation is observed with variations in both the cation and anion.

Introduction

The structure of liquids has been studied for many years. Investigations have, in general, been focussed on the arrangements in molecular solvents such as water, *t*-butanol, and simple chlorinated solvents. The field of molten salts and the structures thereof is much less studied, and within this field, the study of the structure of room-temperature ionic liquids is in its infancy. Interest in ionic liquids stems from their properties (including effectively zero vapor pressure) and the ease by which many of these properties may be varied. This area has been the subject of an increasing number of publications concentrating mainly on their use for electrochemical processes or as reaction media, and these have been subject of a number of recent reviews.[1]

A variety of experimental techniques have been used to investigate liquid structure including neutron diffraction, X-ray scattering and extended X-ray absorption fine structure (EXAFS), and NMR spectroscopy. The importance of the elucidation of liquid structures is clear because this gives an indication as to which interactions are important within the phase and, therefore, which dominate many chemical and physical properties of the liquid, for example, solvation, density, viscosity, and polarity. With respect to the study of molten salt/ionic liquid structure, Enderby and co-workers were the pioneers and clearly demonstrated that the structure of molten NaCl, for example, was dominated by alternating anion and cation interactions.[2] In this case, the local order extended out to three to four anion–cation pairs and the molten salt is a highly structured liquid. Since this time, experimental determination of ionic media has expanded significantly with the examination of a wide range of single-component and two-component salts.

Neutron diffraction has been used to examine the structure of alkali haloaluminates of the type $(MX)_y(AlX_3)_{1-y}$, where M is an alkali metal and X is a halogen (Cl or Br).[3] For KBr- and KCl-based systems where $y = 0.25$ and 0.33, the diffraction clearly showed good agreement with Raman and infrared data[4] in that for both bromide and chloride salts, $[Al_2X_7]^-$ anions dominated the aluminium speciation. Furthermore, strong agreement was found between the liquid structure and crystal structures of related materials such as $K[Al_2Br_7]$. Badyal et al. also examined the structure of binary mixtures of $AlCl_3$ and NaCl and LiCl from excess to a 1:1 mixture.[5] In this case, as the mixture became more ionic, that is, with the addition of the alkali halide, the number of Al–Cl–Al linkages decreased resulting in the formation of $[AlCl_4]^-$ species. Importantly, this also coincided with a decrease in the long range order within the liquid despite the presence of a high degree of charge ordering in the system. The structure proposed from neutron scattering was in good agreement with the X-ray diffraction performed by Takahashi et al.[6] on 1:1 binary mixtures of $AlCl_3$ with LiCl and NaCl. Therein, long-range order was found in the liquid with $[AlCl_4]^-$ tetrahedra surrounding a central $[AlCl_4]^-$ anion at distances of 6.75 and 6.98 Å for LiCl and NaCl, respectively. X-ray diffraction was also employed by Igarashi et al.[7] to examine the liquid structure of a LiF–NaF–KF eutectic mixture. For the ion pairs Li–F, Na–F, and K–F, the nearest neighbor coordination and distances were almost identical to those found in the individual melts of the component salts.

Ionic liquids have also been examined, namely, $AlCl_3$–*N*-butylpyridinium chloride,[8] $AlCl_3$/1-ethyl-3-methylimida-

Chris Hardacre is a Professor of Physical Chemistry in Queen's University Belfast. His current interests include the understanding of gas- and liquid-phase catalytic processes for emission control, clean energy production, and fine chemical synthesis, as well as the study and use of ionic liquids. In the latter, a particular interest is in the determination of structural properties of ionic liquids and solute–solvent interactions.

John Holbrey is a senior research fellow whose research interests include developing clean, atom-efficient approaches to ionic liquid synthesis and understanding the relationship between the solid and liquid structures of ionic liquid materials in addition to the application of ionic liquids as solvents for separations, metal ion complexation, coordination, and catalysis.

Mark Nieuwenhuyzen is a research officer within the School of Chemistry and Chemical Engineering in Queen's University Belfast interested in intermolecular interactions, how they influence the structure of crystalline and liquid materials, and their application to the control of properties in new materials.

Tristan Youngs has been a postdoctoral fellow at Queen's University Belfast since 2004 and works with both the Atomistic Simulation Centre in Physics and the School of Chemistry and Chemical Engineering, studying the solvation of various small molecules by ionic liquids using simulations. In particular, his interests lie in the structural motifs that exist within the liquid phase and relationship between theory and experimental data.

* Corresponding author. Tel: +44 28 9097 4592. Fax: +44 28 9097 4687. E-mail: c.hardacre@qub.ac.uk.
† School of Chemistry and Chemical Engineering.
‡ The QUILL Centre.
§ School of Maths and Physics.

10.1021/ar700068x CCC: $37.00
Published on Web 06/21/2007

zolium chloride ([C_2mim]Cl),[9] HCl/1-ethyl-3-methylimidazolium chloride Cl,[10,11] and $AlCl_3$/LiSCN[12] mixtures. In these cases, X-ray and neutron scattering provided information about the specific interactions between the anions and cations; however, little data about the long-range correlation beyond the first coordination sphere is described. For example, in the mixtures containing HCl and [C_2mim]Cl, first-order differences using hydrogen/deuterium substitution on both the imidazolium ring and the HCl indicated the presence of $[HCl_2]^-$ as an asymmetric species. In the case of $AlCl_3$/LiSCN liquids, the aluminium was modeled with tetrahedral coordination by three chlorines and an isocyanate group. This complex clearly showed that the nitrogen coordinated (as opposed to sulfur) forming an $AlCl_3NCS^-$ species, which is consistent with a hard base–hard acid interaction compared with the softer sulfur donation. A symmetric tetrahedral chloride environment was also found around the lithium. X-ray diffraction has been used to examine the liquid structure of binary ionic liquids of 1,3-dialkylimidazolium fluoride with HF.[13] Again, the solid state and liquid structures are closely related with each showing the presence of the $[HF_2]^-$ anion. In contrast, Shodai et al. reported that the structure of liquid $[(CH_3)_4N]F{\cdot}n$HF ($n = 3$–5) had a range of anion structures of the form $[(HF)_xF]^-$ ($x = 1$–3). In this case, structures with $x = 4$ or 5 were not found in the liquid phase although similar compositions have been found in the solid state.[14]

In contrast with X-ray and neutron scattering, to date, EXAFS has only been used to examine the structure of high-temperature molten salts in detail. EXAFS has a number of limitations with regard to the study of liquid structure, in that it is restricted in the coordination shell that can be examined but conversely can give specific information about an X-ray absorbing center. The detailed arrangement of atoms within coordinated complexes contained by the molten salts can be determined. In this respect, Crozier et al. reported the use of EXAFS to examine the detailed manganese and bromine coordination within the structure of solid and liquid $[Bu_4N][MnBr_3]$ and $[Bu_4N]_2[MnBr_4]$ between room temperature and 400 K.[15] In the molten state, Mn–Br bond distances of 2.46 and 2.50 Å were found for $[Bu_4N][MnBr_3]$ and $[Bu_4N]_2[MnBr_4]$, respectively. In addition, approximately three bromines were found to coordinate around the manganese in the liquid state of $[Bu_4N][MnBr_3]$ compared with six for the solid-state structure. The relationship between molten and solid Rb_2ZnCl_4 with $ZnCl_2$/RbCl has also been studied using EXAFS.[16] On melting $ZnCl_2$, zinc is found to have tetrahedrally coordinated chlorines and is linked by those at corner-sharing sites in a weak extended network. In RbCl, significant disorder in the chloride shell around the rubidium is evident and indicates considerable movement of the Rb^+ and Cl^- in the molten state. In the crystal structure of Rb_2ZnCl_4, the chlorine coordination number around the Rb is between 8 and 9, whereas the Zn is found in isolated $[ZnCl_4]^{2-}$ units. In the molten state, the EXAFS also indicates isolated $[ZnCl_4]^{2-}$ units with a chlorine coordination of 7.6 around the Rb. This may be compared with a chlorine coordination of 4.8 in liquid RbCl. The EXAFS clearly shows that the solid and liquid structures of Rb_2ZnCl_4 are similar and that the melt does not rearrange into a simple combination of the component parts. These studies highlight the fact that although there can be good correlation between the liquid- and solid-state structures for some systems, this is not always the case.

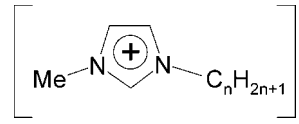

FIGURE 1. Schematic of the 1-alkyl-3-methylimidazolium structure, where for $n = 1$ the structure represents the $[dmim]^+$ cation.

EXAFS analysis has been shown to provide important information concerning the ionic character of the bonding with molten salts. Cu and Br K-edge EXAFS has been used to study the structure of molten CuBr.[17] The fact that there was little contribution to the Cu EXAFS data of Cu–Cu distances and only a small contribution to the Br EXAFS data of Br–Br distances indicated that the melt contained nearly total covalent bonding similar to that found in the solid. Similar results have also been found for AgBr where the liquid state showed almost complete absence of the Ag–Ag correlation distances in the Ag EXAFS data observed in the liquid state.

Our interest has been in understanding the relationship between the crystal and liquid structures of representative room-temperature ionic liquid materials. In addition, the interactions of solutes in ionic liquids have been examined with the ultimate goal of providing insights into the ability of these media to control selectivity, reactivity, and solubility of molecules and catalysts, for example.

Structures of Dimethylimidazolium Salts

A range of 1,3-dimethylimidazolium ($[dmim]^+$) salts have been examined using neutron diffraction as analogues for the longer chain length derivatives.[18–20] These salts are symmetric (Figure 1) and were used in the experimental studies in order to simplify the analysis. Although they have higher melting points than the ionic liquids based on asymmetric alkyl chain substitution on the ring nitrogen atoms, they still provide useful generic information about ionic liquids. Figure 2 shows the probability distribution of chloride around a central imidazolium cation in [dmim]Cl,[17] determined from modeling the neutron data using the empirical potential structural refinement (EPSR) process based on fitting the experimental data with a reverse Monte Carlo procedure.[21] Strong charge ordering was found to be present in this ionic liquid with the anions and cations alternating in the radial distribution function in agreement with that previously reported for alkali halide molten salts. Similarly, probability distribution functions have also been determined for the corresponding ionic liquids with hexafluorophosphate ($[PF_6]^-$)[18] and bis{(trifluoromethyl)sulfonyl}imide ($[NTf_2]^-$)[19] anions as shown in Figure 2. Differences are observed between each of the distributions as a result of

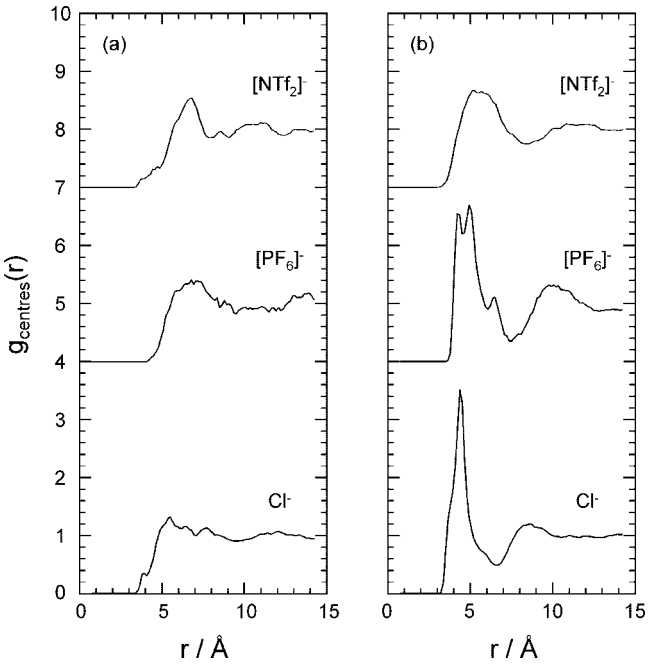

FIGURE 2. Comparison of the partial radial distribution functions for (a) the cation–cation distribution and (b) the cation–anion distribution for the 1,3-dimethylimidazolium chloride, hexafluorophosphate, and bis{(trifluoromethyl)sulfonyl}imide salts derived from the EPSR model. Each radial distribution function is calculated from the center of the imidazolium ring, from the phosphorus atom in the case of $[PF_6]^-$, and from the nitrogen atom in the case of $[NTf_2]^-$.

the differing anions present. An examination of the cation–cation contacts shows that in [dmim]Cl the cations are separated by 5.5 Å, while for the hexafluorophosphate and bis{(trifluoromethyl)sulfonyl}imide analogues, the spacings are 6.3 and 7.0 Å, respectively, that is the cation to cation contacts become larger as the size of the anion is increased, $Cl^- < [PF_6]^- < [NTf_2]^-$. Similarly, the anion–cation distances are expanded with anion size: 4.2 Å (Cl^-), 4.5 Å ($[PF_6]^-$), and 5.2 Å ($[NTf_2]^-$). Although in each case charge ordering was observed, the anion–cation–anion alternating pattern is less pronounced in the case of [dmim][NTf_2] than for either the [dmim]Cl or [dmim][PF_6] liquids as shown by the almost coincident position of the second shells of the cations and anions in [dmim][NTf_2] at ~13 Å.

From the EPSR model, the spatial probability distribution maps of the anions and cations may be examined in detail. These are shown for each ionic liquid in Figure 3, where it is clear that a gradual change is observed in the space that the anions and cations occupy. The main observations are that progressing from chloride to hexafluorophosphate to bis{(trifluoromethyl)sulfonyl}imide, the anions interact less with the ring hydrogens and the cations and anions start to occupy different positions. These effects are the result of the size and charge distribution on the anion changing. The point-charge-like behavior decreases as the anion size increases and the charge becomes more delocalized. This has the effect of reducing the hydrogen bonding accepting ability of the anion, and thus the interaction with the ring hydrogens reduces. A further consequence of this delocalization of

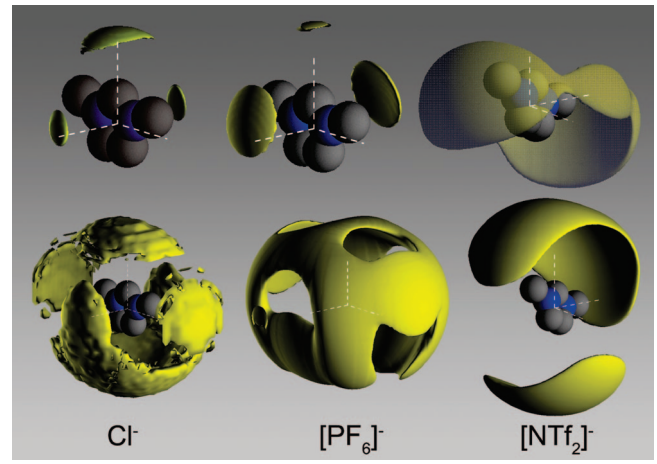

FIGURE 3. Probability distributions of (a) the anions and (b) the imidazolium cations around an imidazolium cation derived from the EPSR model for liquid [dmim]Cl, [dmim][PF_6], and [dmim][NTf_2]. For anion distributions in panel a, the contour level was chosen to enclose the top 5% of the molecules, while for the cation distributions in panel b, the contours enclose the top 20% of molecules each in the distance range 0–9 Å.

the charge is that ionic bonding in the liquid becomes softer and results in increased overlap of the anions and cations in the radial distribution of [dmim][NTf_2]. Moreover, as the anion size increases, the anions and cations must occupy mutually exclusive positions in order to pack most efficiently, and thus it is only in the chloride liquid that an onion-skin structure may be achieved.

As discussed, of key interest is the relationship between the solid-state and liquid structure. In the case of [dmim]Cl and [dmim][PF_6], a remarkable similarity between the reported crystal structure data and the interactions found in the liquids is found. For example, in the solid-state structure of [dmim]Cl, hydrogen–anion contacts dominate the interactions with each cation interacting with six anions, which is also found in the EPSR model of the liquid structure. In the crystal structure, the closest distance between the cations is found to be a van der Waals contact distance between two methyl hydrogens in adjacent cation dimers at 2.5 Å. This is not associated with an attractive interaction, and the anion–cation interactions control the structure, as expected. Importantly, this is the shortest cation–cation distance in the liquid structure. In contrast, a correspondence between the crystal structure and liquid structure is not found for [dmim][NTf_2]. This is most clearly shown by the differences in the conformation of the anion between the solid and liquid states. The bis{(trifluoromethyl)sulfonyl}imide anion can adopt either *cis* or *trans* conformers, shown in Figure 4, and occupies the *cis* form in the crystal.[22] A distribution of forms is found in the liquid with the *trans* most predominant as shown in Figure 5.

The [dmim][NTf_2] crystal structure is unusual because most $[NTf_2]^-$-based structures show the *trans* form. It is possible that the reported structure of [dmim][NTf_2] is only one of a number of polymorphs one of which may match the liquid structure more closely. Polymorphism has been demonstrated for a wide range of ionic liquids,

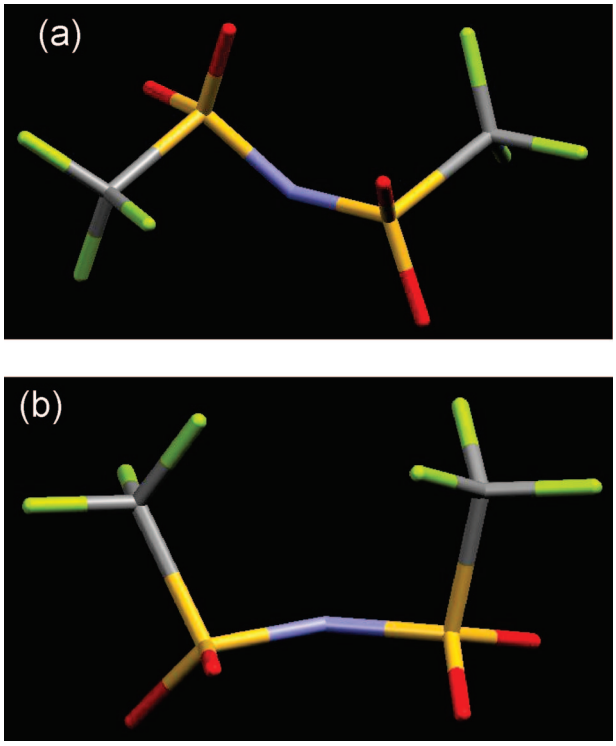

FIGURE 4. Models showing (a) the *trans* and (b) the *cis* conformation of the bis{(trifluoromethyl)sulfonyl}imide anion.

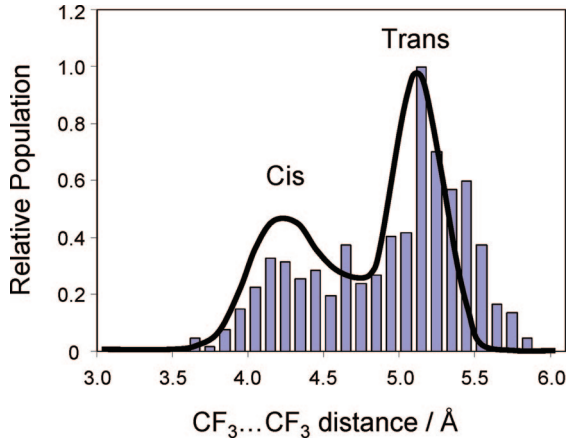

FIGURE 5. Comparison of the distribution of the $CF_3 \cdots CF_3$ distances as a function of the number of anions in liquid [dmim][NTf_2] derived from the EPSR model, shown as bars, with that derived from the molecular force field method developed by Lopes and Padua,[27] shown as a solid line.

for example, 1-alkyl-3-methylimidazolium tetrachloropalladate(II) salts ($[C_n\text{mim}]_2[PdCl_4]$, $n = 10$–18)[23] and short[24] and long[25] alkyl chain halide-based methylimidazolium salts. In the latter, large differences are observed in the structures on heating the salts. These changes are associated with relaxation of alkyl chain conformers in the cation. In the long chain salts, the liquid and the solvent crystallized structures show completely different X-ray scattering patterns with the interlayer spacing being approximately twice as big in the crystal; however, after relaxation the liquid and crystal structures are similar.

Although experimental data on ionic liquid structures is limited, a wide range of simulations have been applied to this media originally pioneered by the seminal work of Lynden-Bell and co-workers.[26] Comparison of simulation data with models produced from the neutron diffraction show good general agreement. For example, Figure 5 shows the *cis*/*trans* distribution of the bis{(trifluoromethyl)sulfonyl}imide anion derived from the EPSR-determined structure from experimental data and that derived from Lopes and Padua using a molecular dynamics simulation combined with a molecular force field approach to obtain the potentials.[27] However, some differences are commonly observed; for example, the simulated data can show greater structuring of the lobe associated with the hydrogen at the C(2) position, whereas the experimental data shows some propensity for anions to position themselves above and below the plane of the imidazolium ring.

The surface structure of long and short alkyl chain length imidazolium-based ionic liquids has also been investigated. With use of neutron and X-ray reflectivity measurements,[28] a lamellar structure of the ionic liquids is found. While this is expected for the long chain materials, which form liquid crystalline phases,[29] segregation for the $[C_4\text{mim}]^+$-based ionic liquids was more surprising. The reflectivity data, as well as sum frequency generation spectroscopy[30] and surface simulations,[31] for example, are valuable in modeling the interaction of ionic liquids with surfaces, which is vital if surface-driven processes such as heterogeneous catalysis[32] or tribological applications[33] are to be understood in detail. Interestingly, this type of behavior has also now been found in simulations where hydrocarbon-rich and ion-rich areas are separated. Although further research needs to be performed in this area, this structural representation of the system provides important data in the control of selectivity and activity for transformations in ionic liquids.

Solute–Solvent Interactions

A good understanding of solute–solvent interactions is vital if a comprehensive understanding of ionic liquid chemistry is to be obtained. This is particularly important where differences arise between reactions performed in ionic liquids and in molecular solvents. An illustration of the effect of the ionic liquid has been shown by the examination of water solvation in ionic liquids using simulation[34] and vibrational spectroscopy.[35] A clear dependence on the dispersion of water in ionic liquids with respect to its concentration has been established. At low concentration, the water is molecularly dispersed, whereas at higher concentrations, aggregated water is also present. In contrast, in mixtures of water in alcohols, for example, the liquid phase separates on a microscopic scale to form hydrophobic regions and hydrophilic regions.[36] This detailed description has provided an explanation as to why some "wet" ionic liquids can stabilize hydrolytically unstable solutes.[37]

Molecular Solutes. Few experimentally determined detailed structures of solute–ionic liquid structures have been reported to date. In most cases, the solvent interac-

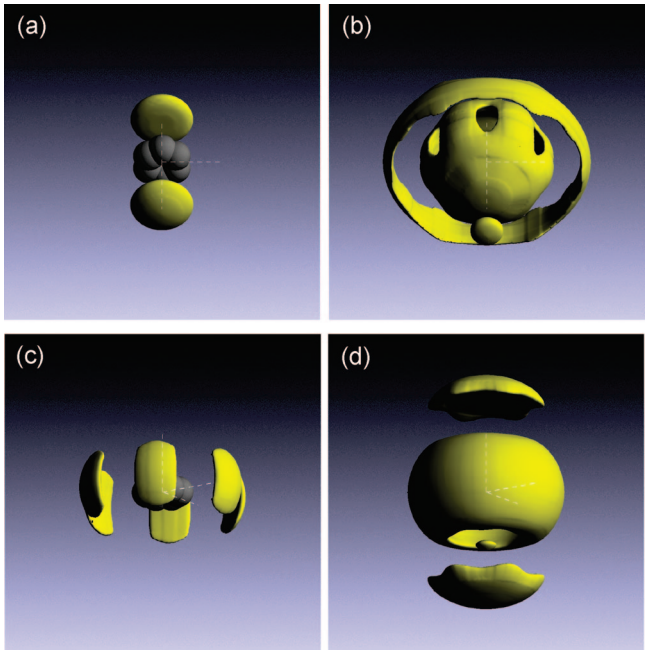

FIGURE 6. Probability distribution of (a, b) the imidazolium cation and (c, d) the hexafluorophosphate anion around a benzene molecule derived from the EPSR model in a mixture containing 1:2 [dmim][PF_6]/benzene. For distributions a and c, the contour level was chosen to enclose the top 5% of the ions in the distance range 0–8 Å, while for distributions b and d, the contours enclose the top 25% of ions in the distance range 0–12 Å.

tion with the solute has been examined rather than the effect of the solute on the extended structure of the solvent. The latter has been probed using neutron scattering for mixtures of benzene with [dmim][PF_6].[38] As expected, the addition of the solute expands the ion–ion structure; however, more surprisingly, the long-range charge ordering in the system is still present. This is a consequence of the distinct ordering of the ions around the benzene. Figure 6 shows the spatial distribution of $[PF_6]^-$ anions and $[dmim]^+$ cations around a benzene molecule derived from the EPSR simulation. Figure 6a,c represent the spatial distribution of the ions in the first coordination shell around a central benzene molecule. In this first shell, the anions are found in the plane of the benzene ring interacting with the slightly positively charged ring hydrogens, whereas the cations are found above and below the aromatic ring interacting with the electron-rich π-system. In the second coordination shell, shown in Figure 6b,d for the cation and anion, respectively, the positions of the ions reverse with the anions above and below the ring and the cations in the plane of the ring. This is due to the cation–anion charge ordering forming the alternating charge-ordered structure found in the pure ionic liquid. Molecular dynamics simulations of this system have also been examined by Lynden-Bell and coworkers.[39] Similar distributions were found around the benzene molecule. Moreover, for the higher order shells, alternating cation–anion layers are still observed. As found with other comparisons of theory and experiment, some differences are observed, and these relate to the changes in structure with benzene concentration. In the simulations, the same structure was observed irrespective of whether one benzene, 33 mol % benzene, or 67 mol % benzene was present in the simulation box. In contrast, the EPSR model of the neutron data only showed clearly defined distributions for the cations/anions where the ion–ion interactions were minimized, that is, in benzene-rich samples.

As with the pure solvents, it is informative to compare crystal structures with the liquid structure where appropriate. A crystal structure has been obtained for [dmim][PF_6]·0.5C_6H_6, which shows clathrate behavior with the benzene molecules occupying channels in the salt crystal.[40] A comparison of the structure of the solid for the benzene incorporated and pure salt material shows that there is a huge reorganization of the cations, and this is clear from the liquid structure in the cation spatial distribution pattern. Furthermore, as found in the molten state of the benzene with [dmim][PF_6], short contacts are also found between the cation hydrogens and the benzene hydrogens in the crystal structure dominated by the methyl hydrogen contacts. Despite these similarities between the liquid and solid-state structures, the correlation between the phases is weak in comparison with that found for the pure salt and is likely to reflect the increased complexity of the system. Lachwa et al. have also been able to relate inclusion compounds in [C_2mim][NTf_2]–benzene mixtures to their phase behavior and postulate at least three different structures present in the liquid dependant on the solute concentration.[41] This shows the importance of the relative ratio of ion–ion, ion–solute, and solute–solute interactions as discussed in the case of [dmim][PF_6] and benzene.[37]

As well as benzene, glucose has been examined in [dmim]Cl.[42] This is of particular interest due to the discovery that cellulose dissolved in the IL 1-methyl-3-butylimidazolium chloride at high concentrations.[43] The subsequent ionic liquid process allows facile material manufacture of cellulosic products and the possible replacement of the solvents traditionally employed, which have high environmental impact. In this case, neutron scattering experiments were used to validate molecular dynamics simulations, which provided a detailed picture of the glucose–ionic liquid interaction used as an analogue for the practical system.

Figure 7 illustrates the probability distribution of chloride ions around a glucose molecule from a molecular dynamics simulation of 96 [dmim]Cl ion pairs and a single glucose molecule. The chlorides, shown in red, are found to hydrogen bond to the hydroxyls in the glucose, denoted O1, O2, O3, O4, and O6. In contrast, the cations are only found to bind weakly to the solute, and thus the anion interaction is of primary importance in the solubilization of the solute. On average, the number of hydrogen bonds to the glucose is more than the coordination number of anions around the solute within a radius of 6.0 Å. Using a chronological map of H-bonds between specific chloride anions and glucose hydroxyl groups, one can determine the number of hydrogen bonds involving the glucose molecule and average coordination number. Taking the

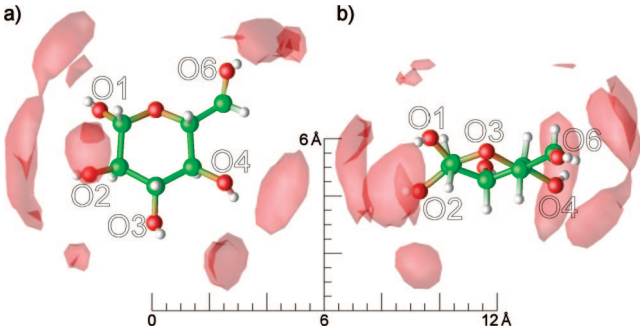

FIGURE 7. Two views, (a) top face of molecule and (b) looking down onto the ring oxygen, of the three-dimensional spatial distribution of chloride anions around the glucose molecule in the chair conformation. The distribution was calculated in the local frame of the glucose and drawn at five times the bulk density from the molecular dynamics simulation of a single glucose molecule in 96 [dmim]Cl ion pairs. Reprinted with permission from ref 42. Copyright 2006 Wiley-VCH.

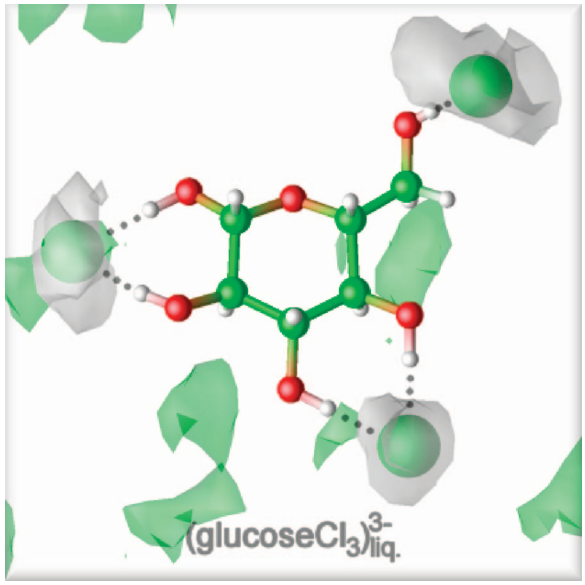

FIGURE 8. Probability distribution of chloride around glucose showing the structure associated with a 3:5 chloride/hydroxyl ratio calculated in the local frame of the glucose and drawn at five times the bulk density from the molecular dynamics simulation of a single glucose molecule in 96 [dmim]Cl ion pairs. Reprinted with permission from ref 42. Copyright 2006 Wiley-VCH.

definition that only Cl···O distances <3.5 Å and Cl···H–O angle >150.0° constitute hydrogen bonds, on average 4.39 hydrogen bonds are formed compared with 3.86 anions in the first shell. The consequence of this is that some of the hydroxyls must be bridge bound to anions as shown in Figure 8 for a 3:5 chloride/hydroxyl ratio. Overall, the most common configuration is a 4:5 chloride/hydroxyl ratio where only one anion "bridges" two hydroxyl groups. These simulations were performed using a single solute molecule in 96 [dmim]Cl ion pairs. However, the potentials used are consistent with the neutron scattering data. This is shown by the excellent agreement between experimental and simulated curves in terms of peak position and the overall shape of the data in Figure 9 for a much higher concentration of glucose, namely, a 1:5 glucose/solvent mixture. Preliminary analysis of this data shows that the effect of the increased glucose concentration has

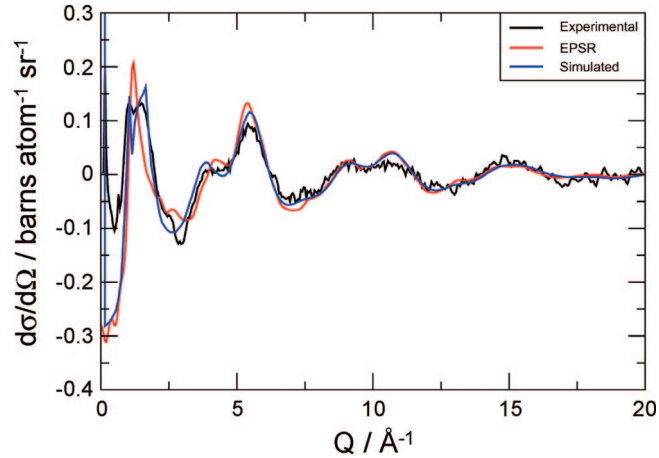

FIGURE 9. Total structure factors from a 1:5 glucose/[dmim]Cl solution as measured by small-angle neutron scattering (black), the fit to data from the empirical potential structure refinement procedure (red), and the calculated curve from molecular dynamics simulations (blue). Reprinted with permission from ref 42. Copyright 2006 Wiley-VCH.

variable influence on the ionic liquid structure. The immediate cation–anion interaction remains largely unaffected by the inclusion of the glucose in the system. Small differences in the second anion shell in the radial distribution function are observed with this peak decreasing in intensity due to the presence of the glucose interrupting the alternating cation–anion structure of the ionic liquid. A similar decrease is also found in the intensity of the first peak in the anion–anion radial distribution function compared with that of the pure ionic liquid.

For this system, although there are no crystallographic data available, NMR has been used to examine the local interactions between glucose and [C_4mim]Cl.[44] In agreement with the simulation, the cations do not interact strongly with the solute, and the main interaction is with the anion. Remsing et al. used the variation of $^{35/37}$Cl NMR line broadening as a function of the glucose concentration to estimate the coordination number of the anions. A significant difference between the simulation, and the NMR data is found with the latter showing a 1:1 correlation of hydroxyls with anions compared with a calculated value of ~5:4. It has been suggested that this difference may be associated with the determination of a coordination number compared with the number of hydrogen bonds. The NMR data is not sensitive enough to distinguish between two OH groups hydrogen bonding to two separate chlorides and two OH groups bound to the same chloride and thus overestimates the coordination number.

In both studies, the importance of anion–solute interactions has been clearly shown by theory and spectroscopy for a range of solutes. Due to the large number of atoms in most ionic liquids and the fact that neutron scattering relies on the contrast between samples with isotopically exchanged atoms, in particular, hydrogen/deuterium, to provide a number of scattering profiles that may be fitted and analyzed, the number of systems that can be studied practically is limited. Currently, to enable a difference to be observed between samples, 2–3% of the

total number of atoms in a sample must be H–D exchanged, for example. If the purpose of the experiment is to investigate the solute–solvent interaction, the exchangeable atoms should also be on the solute. Obviously, the contrast is greatest where the difference in neutron scattering length between the isotopes is greatest, and hence, H–D exchange is most commonly used. X-ray scattering patterns may also be used to supplement the data and will provide useful information regarding heavy solutes. Therefore, the neutron scattering is limited to samples where high mole fractions of solutes are possible and that can undergo isotopic exchange where the difference in the neutron scattering length is high. Clearly, if the solute causes a large change in the ionic liquid structure this can be probed without the need to use isotopically exchanged solutes.

Dissolved Metal Complexes. EXAFS has been extensively employed to examine the structure of metal complexes in both first and second generation ionic liquids both *in situ* during reactions and *ex situ*.[45] Dent et al. were among the first to employ the technique to study the dissolution of $[C_2mim][MCl_4]$ in $[C_2mim]Cl–AlCl_3$ binary mixtures, for M = Mn, Co, and Ni, as a function of $AlCl_3$ mole fractions.[46] Importantly, this study showed the noninnocent nature of the ionic liquid on the dissolved species for the first time. Therein, the coordination of Ni, Co, and Mn was found to change from $[MCl_4]^{2-}$ to $[M(AlCl_3)_4]^-$ as the mole fraction of $AlCl_3$ increased.

Our interest has been to examine the speciation of complexes during and following reaction using EXAFS. For example, the catalytically active species formed during the Ni-catalyzed dimerization of but-1-ene in a range of chloroaluminate ionic liquids has been studied in detail.[47] *In situ* Ni K-edge data was taken for $NiCl_2(PiPr_3)_2$ and $[Ni(MeCN)_6][BF_4]_2$ in basic and acidic chloroaluminate ionic liquids using mixtures of $AlCl_3$ and $[C_2mim]Cl$ in the absence and presence of ethylaluminium chloride and correlated with the reaction kinetics. Irrespective of the system examined here, $[Ni[AlCl_4]_3]^-$ was found in all the solutions that showed high activity over extended reaction times. Deactivation of the catalysts over time was attributable to the gradual transformation to an inactive tetrachloronickel species or by reduction to metallic nickel.

The Heck reaction catalyzed by palladium salts and complexes in room-temperature ionic liquids has also been examined in detail using *in situ* EXAFS.[46,48] In this case, the importance of correlating the structural data with the reaction kinetics was clearly illustrated. For example, on dissolution of palladium acetate in non-halide-based ionic liquids formation of ~1 nm palladium nanoparticles, which showed good activity, was observed, as shown by the pseudo-radial distribution functions in Figure 10. In constrast dissolution in chloride-based ionic liquids resulted in the formation of $[PdCl_4]^{2-}$ in general, as shown for the ionic liquid 1-hexyl-2,3-dimethyl imidazolium chloride

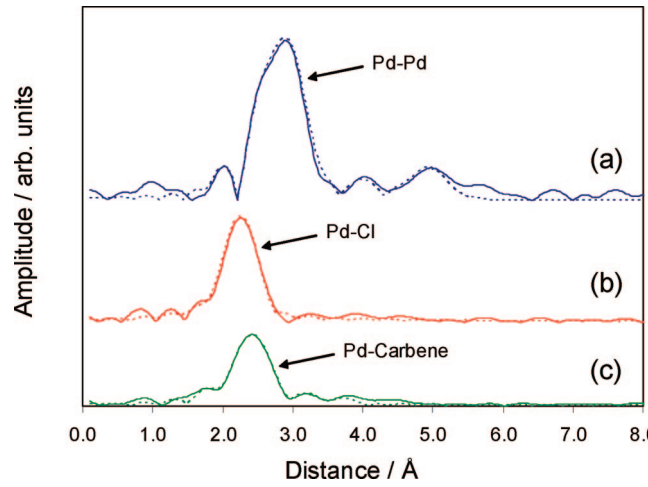

FIGURE 10. Comparison of the experimental (solid line) and fitted (dashed line) pseudo-radial distribution functions from palladium acetate dissolved in (a) $[C_4mim][PF_6]$, (b) $[C_6mmim]Cl$, and (c) $[C_6mim]Cl$ at 80 °C.

($[C_6mmim]Cl$) in Figure 10c. In this ionic liquid, the C(2) position is capped by a methyl group; however, in 1-hexyl-3-dimethyl imidazolium chloride ($[C_6mim]Cl$), this position is occupied by an acidic hydrogen, which can be abstracted by the base present in the Heck reaction and results in the the formation of a *bis*-carbene palladium complex. The Heck reaction in the chloride-based ionic liquids showed poor reactivity but in the presence of the reagents did gradually form palladium metal, and at this point, the reaction was initiated. The correlation between the induction period and the nanoparticle formation was strong, and although the metal may not be the active site for the catalysis,[49] the presence of Pd(0) is clearly important. Carbene complexes have also been identified by EXAFS in the Suzuki reaction catalyzed by $[NiCl_4]^{2-}$-based ionic liquids.[50] Interestingly, in this case, Zhong *et al.* showed that pretreatment with base prior to reaction to form the carbene complex improved the reaction.

EXAFS has also been invaluable in understanding speciation of actinides and lanthanides in ionic liquids.[51] For example, in the extraction of heavy metals from aqueous streams using ionic liquids, the mechanism of the separation has been examined in detail.[52] EXAFS has been used to understand the coordination of uranium using extractants such as carbamoylphosphine oxide (CMPO) and tri(*n*-butyl)phosphate. In $[C_4mim][PF_6]$ or $[C_8mim][NTf_2]$ as the extracting solvent, two uranium species are formed both containing uranyl oxygens with either 4–4.5 equatorial oxygens or the formation of $[UO_2(NO_3)(CMPO)]^+$. In contrast, in dodecane complexes with six equatorial oxygens due to the coordination of two monodentate CMPO molecules (P=O bound) and two bidentate nitrate anions were observed. The difference was attributed to the coordination of water. From the data, a mechanism whereby ionic liquid cation exchange with ions in the aqueous phase was proposed. From EXAFS studies, an analogous mechanism was also proposed for the extraction of Sr^{2+}(aq) using ionic liquids using *cis*-

syn-cis-dicyclohexyl-18-crown-6 as the ligand.[53] In both cases, irrespective of the hydrophobicity of the ionic liquid used, significant dissolution of the ionic liquid in the aqueous phase was found.

The speciation of uranium in the electrochemical reprocessing of nucelar fuel has been studied using UV–vis combined with EXAFS. Following anodization of uranium metal in $[C_2mim]Cl$, the U L_{III}-edge EXAFS showed a mixture of uranium(IV) and uranium(VI) oxidation states corresponding to a 1:1 mixture of $[UCl_6]^{2-}$ and $[UO_2Cl_4]^{2-}$ species.[54] The presence of the high oxidation states was unexpected and was attributed to the presence of water in the ionic liquid. More complex speciation was observed following the oxidative dissolution of uranium(IV) oxide in $[C_4mim][NO_3]$ using concentrated nitric acid as the oxidizing agent.[55] Therein, a dinuclear dioxouranium(VI) salt containing a bridging oxalate ligand, 1-butyl-3-methylimidazolium μ_4-(*O*,*O*,*O*′,*O*′-ethane-1,2-dioato)-bis{bis(nitrato-*O*′,*O*)dioxouranate(VI)} ($[C_4mim]_2[\{UO_2(NO_3)_2\}_2(\mu\text{-}C_2O_4)]$), as well as $UO_2(NO_3)_2{\cdot}6H_2O$ are formed in 15:85 mononuclear nitrate/dinuclear oxalate dimer molar ratio in solution.

It should be noted that although the solvation of metal complexes in ionic liquids has been investigated by a number of groups, further research is needed in order to understand the properties of these systems in, for example, catalysis and electrochemistry. This is particularly true in third generation ionic liquids where few studies have been reported.

Summary

Our understanding of ionic liquid systems both in terms of the structure of the liquid and ionic liquid–solute interaction is becoming more established. Clear charge ordering is found in the ionic liquids; however, as expected, with increased delocalization of the charge in the anion the ionic bonding becomes softer, which results in increasing overlap of the anion/cation coordination shells. In the presence of benzene, the long-range order found in the pure solvent still exists, and the anions and cations initially solvating the molecule in the plane of the benzene and above and below the ring, respectively. For glucose, strong hydrogen bonding between the hydroxyl groups and chloride is observed, which is thought to be the reason the chloride-based ionic liquids are able to dissolve cellulose efficiently. In this case, bridging chloride anions are present in the predominant structure resulting in the 4:5 chloride/hydroxyl ratio being most prevalent. Solvation of metal-containing species in first and second generation ionic liquids shows a wide range of structures and EXAFS has been instrumental in understanding the structure–activity relationships in both catalytic and extractive systems. For example, in the Heck reaction, the reaction was only found to be efficiently catalyzed in the presence of palladium nanoparticles. Therein the growth of the particles directly correlated with the rate of reaction. In the presence of chloride, the palladium was stabilized as either $[PdCl_4]^{2-}$ or a *bis*-carbene complex, which prevented nanoparticle growth and resulted in low activity for the Heck coupling process. However, despite the insight gained from these studies, the number of experimental reports is still relatively low compared with theoretical studies. Although there is still a lack of experimentally determined data available that may be compared with the simulations, where it exists, there appears to be good agreement between the theory and experiment.

We wish to thank the EPSRC for financial support under a portfolio partnership.

References

(1) *Ionic Liquids in Synthesis*, Wasserscheid, P., Welton T., Eds., Wiley-VCH Verlag: Weinheim, Germany, 2003. Silvester, D. S.; Compton, R. G. Electrochemistry in room temperature ionic liquids: A review and some possible applications. *Z. Phys. Chem.* **2006**, *220*, 1247–1274. Endres, F.; El Abedin, S. Z. Air and water stable ionic liquids in physical chemistry. *Phys. Chem. Chem. Phys.* **2006**, *8*, 2101–2116. Harper, J. B.; Kobrak, M. N. Understanding organic processes in ionic liquids: Achievements so far and challenges remaining. *Mini-Rev. Org. Chem.* **2006**, *3*, 253–269.

(2) Edwards, F. G.; Enderby, J. E.; Howe, R. A.; Page, D. I. Structure of molten sodium-chloride. *J. Phys. C* **1975**, *8*, 3483–3490. Biggin, S.; Enderby, J. E. Comments on the structure of molten-salts. *J. Phys. C* **1982**, *15*, L305–309.

(3) Blander, M.; Bierwagen, E.; Calkins, K. G.; Curtiss, L. A.; Price, D. L.; Saboungi, M.-L. Structure of acidic haloaluminate melts—neutron-diffraction and quantum chemical calculations. *J. Chem. Phys.* **1992**, *97*, 2733–2741.

(4) Cyvin, S. J.; Klaboe, P.; Rytter, E.; Øye, H. A. Spectral evidence for $Al_2Cl_7^-$ in chloride melts. *J. Chem. Phys.* **1970**, *52*, 2776–2778. Hvistendahl, J.; Klaboe, P.; Rytter, E.; Øye, H. A. Infrared-emission spectra of alkali chloroaluminates and related melts. *Inorg. Chem.* **1984**, *23*, 706–715.

(5) Badyal, Y. S.; Allen, D. A.; Howe, R. A. The structure of liquid $AlCl_3$ and structural modification in $AlCl_3$–MCl (M = Li, Na) molten-salt mixtures. *J. Phys.: Condens. Matter* **1994**, *6*, 10193–10220.

(6) Takahashi, S.; Maruoka, K.; Koura, N.; Ohno, H. X-ray-diffraction analysis of molten $AlCl_3$-NaCl system. *J. Chem. Phys.* **1986**, *84*, 408–415. Takahashi, S.; Muneta, T. N.; Koura, N.; Ohno, H. Structural-analysis of the molten-salt 50 mol-percent $AlCl_3$-50 mol-percent NaCl by X-ray-diffraction. *J. Chem. Soc., Faraday Trans. II* **1985**, *81*, 1107–1115.

(7) Igarashi, K.; Okamoto, Y.; Mochinaga, J.; Ohno, H. X-ray-diffraction study of molten eutectic LiF-NaF-KF mixture. *J. Chem. Soc., Faraday Trans. I* **1988**, *84*, 4407–4415.

(8) Takahashi, S.; Koura, N.; Murase, M.; Ohno, H. Structural-analysis of $AlCl_3$-n-butylpyridinium chloride electrolytes by X-ray-diffraction. *J. Chem. Soc., Faraday Trans. II* **1986**, *82*, 49–60.

(9) Takahashi, S.; Suzuya, K.; Kohara, S.; Koura, N.; Curtiss, L.A.; Saboungi, M.-L. Structure of 1-ethyl-3-methylimidazolium chloroaluminates: Neutron diffraction measurements and ab initio calculations. *Z. Phys. Chem.* **1999**, *209*, 209–221.

(10) Truelove, P. C.; Haworth, D.; Carlin, R. T.; Soper, A. K.; Ellison, A. J. G.; Price, D. L. *Proceedings of the 9th International Sympopsium on Molten Salts, San Francisco*; Electrochem. Soc.: Pennington, NJ, 1994; Vol. *3*, pp 50–57.

(11) Trouw, F. R.; Price, D. L. Chemical applications of neutron scattering. *Annu. Rev. Phys. Chem.* **1999**, *50*, 571–601.

(12) Lee, Y.-C.; Price, D. L.; Curtiss, L. A.; Ratner, M. A.; Shriver, D. F. Structure of the ambient temperature alkali metal molten salt $AlCl_3$/LiSCN. *J. Chem. Phys.* **2001**, *114*, 4591–4594.

(13) Hagiwara, R.; Matsumoto, K.; Tsuda, T.; Ito, Y.; Kohara, S.; Suzuya, K.; Matsumoto, H.; Miyazaki, Y. The structures of alkylimidazolium fluorohydrogenate molten salts studied by high-energy X-ray diffraction. *J. Non-Cryst. Solids* **2002**, *312–314*, 414–418. Matsumoto, K.; Hagiwara, R.; Ito, Y.; Kohara, S.; Suzuya, K. Structural analysis of 1-ethyl-3-methylimidazolium bifluoride melt. *Nucl. Instrum. Methods Phys. Res., Sect. B* **2003**, *199*, 29–33.

(14) Shodai, Y.; Kohara, S.; Ohishi, Y.; Inaba, M.; Tasaka, A. Anionic species $(FH)_xF^-$ in room-temperature molten fluorides $(CH_3)_4NF{\cdot}m$HF. *J. Phys. Chem. A* **2004**, *108*, 1127–1132.

(15) Crozier, E. D.; Alberding, N.; Sundheim, B. R. EXAFS study of bromomangante ions in molten salts. *J. Chem. Phys.* **1983**, *79*, 939–943.

(16) Li, H. F.; Lu, K. Q.; Wu, Z. H.; Dong, J. EXAFS studies of molten $ZnCl_2$, RbCl, and Rb_2ZnCl_4. *J. Phys. Condens. Matter* **1994**, *6*, 3629–3640. Lu, K. Q.; Li, H. F.; Wu, Z. H.; Dong, J.; Cheng, Z. N. Structural studies of some chloride melts with EXAFS. *Physica B* **1995**, *208&209*, 339–343.

(17) Di Cicco, A.; Minicucci, M.; Filipponi, A. New advances in the study of local structure of molten binary salts. *Phys. Rev. Lett.* **1997**, *78*, 460–463. Minicucci, M.; Di Cicco, A. Short-range structure in solid and liquid CuBr probed by multiple-edge X-ray-absorption spectroscopy. *Phys. Rev. B* **1997**, *56*, 11456–11464. Di Cicco, A. Local structure in binary liquids probed by EXAFS. *J. Phys. Condens. Matter* **1996**, *8*, 9341–9345.

(18) Hardacre, C.; Holbrey, J. D.; McMath, S. E. J.; Bowron, D. T.; Soper, A. K. Structure of molten 1,3-dimethylimidazolium chloride using neutron diffraction. *J. Chem. Phys.* **2003**, *118*, 273–278.

(19) Hardacre, C.; McMath, S. E. J.; Nieuwenhuyzen, M.; Bowron, D. T.; Soper, A. K. Liquid structure of 1, 3-dimethylimidazolium salts. *J. Phys. C* **2003**, *15*, S159–S166.

(20) Deetlefs, M.; Hardacre, C.; Nieuwenhuyzen, M.; Padua, A. A. H.; Sheppard, O.; Soper, A. K. Liquid structure of the ionic liquid 1,3-dimethylimidazolium bis{(trifluoromethyl)sulfonyl}amide. *J. Phys. Chem. B* **2006**, *110*, 12055–12061.

(21) Soper, A. K. Empirical potential Monte Carlo simulation of fluid structure. *Chem. Phys.* **1996**, *202*, 295–306. Soper, A. K. The radial distribution functions of water and ice from 220 to 673 K and at pressures up to 400 MPa. *Chem. Phys.* **2000**, *258*, 121–136. Soper, A. K. Tests of the empirical potential structure refinement method and a new method of application to neutron diffraction data on water. *Mol. Phys.* **2001**, *99*, 1503–1516.

(22) Holbrey, J. D.; Reichert, W. M.; Rogers, R. D. Crystal structures of imidazolium bis(trifluoromethanesulfonyl)imide 'ionic liquid' salts: the first organic salt with a cis-TFSI anion conformation. *Dalton Trans.* **2004**, 2267–2271.

(23) Hardacre, C.; Holbrey, J. D.; McCormac, P. B.; McMath, S. E. J.; Nieuwenhuyzen, M.; Seddon, K. R. Crystal and liquid crystalline polymorphism in 1-alkyl-3-methylimidazolium tetrachloropalladate(II) salts. *J. Mater. Chem.* **2001**, *11*, 346–350.

(24) Hamaguchi, H.; Saha, S.; Ozawa, R.; Hayashi, S. Raman and X-ray studies on the structure of [bmim]X (X=Cl, Br, I, $[BF_4]$, $[PF_6]$): Rotational isomerism of the $[bmim]^+$ cation. *ACS Symp. Ser.* **2005**, *901*, 68–78. Ozawa, R.; Hayashi, S.; Saha, S.; Kobayashi, A.; Hamaguchi, H. Rotational isomerism and structure of the 1-butyl-3-methylimidazolium cation in the ionic liquid state. *Chem. Lett.* **2003**, *32*, 948–949.

(25) Downard, A.; Earle, M. J.; Hardacre, C.; McMath, S. E. J.; Nieuwenhuyzen, M.; Teat, S. J. Structural studies of crystalline 1-alkyl-3-methylimidazolium chloride salts. *Chem. Mater.* **2004**, *16*, 43–48.

(26) Hanke, C. G.; Price, S. L.; Lynden-Bell, R. M. Intermolecular potentials for simulations of liquid imidazolium salts. *Mol. Phys.* **2001**, *99*, 801–809.

(27) Lopes, J. N. C.; Padua, A. A. H. Molecular force field for ionic liquids composed of triflate or bistrifylimide anions. *J. Phys. Chem. B* **2004**, *108*, 16893–16898.

(28) Bowers, J.; Vergara-Gutierrez, M. C.; Webster, J. R. P. Surface ordering of amphiphilic ionic liquids. *Langmuir* **2004**, *20*, 309–312. Solutskin, E.; Ocko, B. M.; Taman, L.; Kuzmenko, I.; Gog, T.; Deutsch, M. Surface, layering in ionic liquids: An X-ray reflectivity study. *J. Am. Chem. Soc.* **2005**, *127*, 7796–7804. Carmichael, A. J.; Hardacre, C.; Holbrey, J. D.; Nieuwenhuyzen, M.; Seddon, K. R. Molecular layering and local order in thin films of 1-alkyl-3-methylimidazolium ionic liquids using X-ray reflectivity. *Mol. Phys.* **2001**, *99*, 795–800.

(29) Bradley, A. E.; Hardacre, C.; Holbrey, J. D.; Johnston, S.; McMath, S. E. J.; Nieuwenhuyzen, M. Small-angle X-ray scattering studies of liquid crystalline 1-alkyl-3-methylimidazolium salts. *Chem. Mater.* **2002**, *14*, 629–635. De Roche, J.; Gordon, C. M.; Imrie, C. T.; Ingram, M. D.; Kennedy, A. R.; Lo Celso, F.; Triolo, A. Application of complementary experimental techniques to characterization of the phase behavior of $[C_{16}mim][PF_6]$ and $[C_{14}mim][PF_6]$. *Chem. Mater.* **2003**, *15*, 3089–3097. Busico, V.; Corradini, P.; Vacatello, M. Thermal-behavior and observation of a smectic phase in *n*-pentadecylammonium chloride. *J. Phys. Chem.* **1982**, *86*, 1033–1034. Busico, V.; Cernicchlaro, P.; Corradini, P.; Vacatello, M. Polymorphism in anhydrous amphiphilic systems. Long-chain primary *n*-alkylammonium chlorides. *J. Phys. Chem.* **1983**, *87*, 1631–1635. Abdallah, D. J.; Robertson, A.; Hsu, H.-F.; Weiss, R. G. Smectic liquid-crystalline phases of quaternary group VA (especially phosphonium) salts with three equivalent long *n*-alkyl chains. How do layered assemblies form in liquid-crystalline and crystalline phases? *J. Am. Chem. Soc.* **2000**, *122*, 3053–3062.

(30) Rivera-Rubero, S.; Baldelli, S. Surface characterization of 1-butyl-3-methylimidazollum Br^-, I^-, PF_6^-, BF_4^-, $(CF_3SO_2)_2N^-$, SCN^-, $CH_3SO_3^-$, $CH_3SO_4^-$, and $(CN)_2N^-$ ionic liquids by sum frequency generation. *J. Phys. Chem. B* **2006**, *110*, 4756–4765.

(31) Lynden-Bell, R. M.; Del Popolo, M. Simulation of the surface structure of butylmethylimidazolium ionic liquids. *Phys. Chem. Chem. Phys.* **2006**, *8*, 949–954.

(32) Anderson, K.; Goodrich, P.; Hardacre, C.; Rooney, D. W. Heterogeneously catalysed selective hydrogenation reactions in ionic liquids. *Green Chem.* **2003**, *5*, 448–453. Shen, H.-Y.; Judeh, Z. M. A.; Chiang, C. B.; Xia, Q.-H. Comparative studies on alkylation of phenol with tert-butyl alcohol in the presence of liquid or solid acid catalysts in ionic liquids. *J. Mol. Catal. A* **2004**, *212*, 301–308. Hardacre, C.; Mullan, E. A.; Rooney, D. W.; Thompson, J. M.; Yablonsky, G. S. Comparison of mass transfer effects in the heterogeneously catalysed hydrogenation of phenyl acetylene in heptane and an ionic liquid. *Chem. Eng. Sci.* **2006**, *61*, 6995–7006. Pârvulescu, V. I.; Hardacre, C. Catalysis in Ionic Liquids. *Chem. Rev.* **2007**, *107*, in press, and references therein, 10.1021/cr050948h.

(33) Liu, W. M.; Ye, C. F.; Gong, Q. Y.; Wang, H. Z.; Wang, P. Tribological performance of room-temperature ionic liquids as lubricant. *Tribol. Lett.* **2002**, *13*, 81–85.

(34) Hanke, C. G.; Lynden-Bell, R. M. A simulation study of water–dialkylimidazolium ionic liquid mixtures. *J. Phys. Chem. B* **2003**, *107*, 10873–10878.

(35) Cammarata, L.; Kazarian, S. G.; Salter, P. A.; Welton, T. Molecular states of water in room temperature ionic liquids. *Phys. Chem. Chem. Phys.* **2001**, *3*, 5192–5200.

(36) Bowron, D. T.; Finney, J. L.; Soper, A. K. Structural investigation of solute-solute interactions in aqueous solutions of tertiary butanol. *J. Phys. Chem. B* **1998**, *102*, 3551–3563.

(37) For example: Farmer, V.; Welton, T. The oxidation of alcohols in substituted imidazolium ionic liquids using ruthenium catalysts. *Green Chem.* **2002**, *4*, 97–102. Doherty, S.; Goodrich, P.; Hardacre, C; Luo, H. K.; Rooney, D. W.; Seddon, K. R.; Styring, P. Marked enantioselectivity enhancements for Diels-Alder reactions in ionic liquids catalysed by platinum diphosphine complexes. *Green Chem.* **2004**, *6*, 63–67. Amigues, E.; Hardacre, C.; Keane, G.; Migaud, M.; O'Neill, M. Ionic liquids - media for unique phosphorus chemistry. *Chem. Commun* **2006**, 72–74.

(38) Deetlefs, M.; Hardacre, C.; Nieuwenhuyzen, M.; Sheppard, O.; Soper, A. K. Structure of ionic liquid–benzene mixtures. *J. Phys. Chem. B* **2005**, *109*, 1593–1598.

(39) Hanke, C. G.; Johansson, A.; Harper, J. B.; Lynden-Bell, R. M. Why are aromatic compounds more soluble than aliphatic compounds in dimethylimidazolium ionic liquids? A simulation study. *Chem. Phys. Lett.* **2003**, *374*, 85–90. Harper, J. B.; Lynden-Bell, R. M. Macroscopic and microscopic properties of solutions of aromatic compounds in an ionic liquid. *Mol. Phys.* **2004**, *102*, 85–94.

(40) Holbrey, J. D.; Reichert, W. M.; Nieuwenhuyzen, M.; Sheppard, O.; Hardacre, C.; Rogers, R. D. Liquid clathrate formation in ionic liquid-aromatic mixtures. *Chem. Commun.* **2003**, 476–477.

(41) Lachwa, J.; Bento, I.; Duarte, M. T.; Lopes, J. N. C.; Rebelo, L. P. N. Condensed phase behavior of ionic liquid-benzene mixtures: congruent melting of a $[emim][NTf_2]{\cdot}C_6H_6$ inclusion crystal. *Chem. Commun.* **2006**, 2445–2447.

(42) Youngs, T. G. A.; Holbrey, J. D.; Deetlefs, M.; Nieuwenhuyzen, M.; Gomes, M. F. C.; Hardacre, C. A molecular dynamics study of glucose solvation in the ionic liquid 1,3-dimethylimidazolium chloride. *ChemPhysChem* **2006**, *7*, 2279–2281.

(43) Swatloski, R. P.; Spear, S. K.; Holbrey, J. D.; Rogers, R. D. Dissolution of cellose with ionic liquids. *J. Am. Chem. Soc.* **2002**, *124*, 4974–4975.

(44) Remsing, R. C.; Swatloski, R. P.; Rogers, R. D.; Moyna, G. Mechanism of cellulose dissolution in the ionic liquid 1-n-butyl-3-methylimidazolium chloride: a ^{13}C and $^{35/37}Cl$ NMR relaxation study on model systems. *Chem. Commun.* **2006**, 1271–1273.

(45) Hardacre, C. Application of EXAFS to molten salts and ionic liquid technology. *Annu. Rev. Mater. Res.* **2005**, *35*, 29–49.

(46) Dent, A. J.; Seddon, K. R.; Welton, T. The structure of halogenometallate complexes dissolved in both basic and acidic room-temperature halogenoaluminate(III) ionic liquids, as determined by EXAFS. *J. Chem. Soc., Chem. Commun.* **1990**, 315–316.

(47) McMath, S. E. J. Structure–reactivity relationships in ionic liquids, Ph.D. thesis, Queen's University Belfast, 2003.

(48) Hamill, N. A.; Hardacre, C.; McMath, S. E. J. In situ XAFS investigation of palladium species present during the Heck reaction in room temperature ionic liquids. *Green Chem.* **2002**, *4*, 139–142.

(49) Phan, N. T. S.; Van Der Sluys, M.; Jones, C. W. On the nature of the active species in palladium catalyzed Mizoroki-Heck and Suzuki-Miyaura couplings - Homogeneous or heterogeneous catalysis, a critical review. *Adv. Synth. Catal.* **2006**, *348*, 609–679, and references therein.

(50) Zhong, C.; Sasaki, T.; Tada, M.; Iwasawa, Y. Ni ion-containing ionic liquid salt and Ni ion-containing immobilized ionic liquid on silica: Application to Suzuki cross-coupling reactions between chloroarenes and arylboronic acids. *J. Catal.* **2006**, *242*, 357–364.

(51) Jensen, M. P.; Neuefeind, J.; Beitz, J. V.; Skanthakumar, S.; Soderholm, L. Mechanisms of metal ion transfer into room-temperature ionic liquids: the role of anion exchange. *J. Am. Chem. Soc.* **2003**, *125*, 15466–15473. Gaillard, C.; Billard, I.; Chaumont, A.; Mekki, S.; Ouadi, A.; Denecke, M. A.; Moutiers, G.; Wipff, G. Europium(III) and its halides in anhydrous room-temperature imidazolium-based ionic liquids: A combined TRES, EXAFS, and molecular dynamics study. *Inorg. Chem.* **2005**, *44*, 8355–8367.

(52) Visser, A. E.; Jensen, M. P.; Laszak, I.; Nash, K. L.; Choppin, G. R.; Rogers, R. D. Uranyl coordination environment in hydrophobic ionic liquids: an in situ investigation. *Inorg. Chem.* **2003**, *42*, 2197–2199.

(53) Jensen, M. P.; Dzielawa, J. A.; Rickert, P.; Dietz, M. L. EXAFS investigations of the mechanism of facilitated ion transfer into a room-temperature ionic liquid. *J. Am. Chem. Soc.* **2002**, *124*, 10664–10665.

(54) Baston, G. M. N.; Bradley, A. E.; Gorman, T.; Hamblett, I.; Hardacre, C.; Hatter, J. E.; Healy, M. J. F.; Hodgson, B.; Lewin, R.; Lovell, K. V.; Newton, G. W. A.; Nieuwenhuyzen, M.; Pitner, W. R.; Rooney, D. W.; Sanders, D.; Seddon, K. R.; Simms, H. E.; Thied, R. C. Ionic liquids for the nuclear industry: A radiochemical, structural, and electrochemical investigation. *ACS Symp. Ser.* **2002**, *818*, 162–177.

(55) Bradley, A. E.; Hardacre, C.; Nieuwenhuyzen, M.; Pitner, W. R.; Sanders, D.; Seddon, K. R.; Thied, R. C. A structural and electrochemical investigation of 1-alkyl-3-methylimidazolium salts of the nitratodioxouranate(VI) anions, $[\{UO_2(NO_3)_2\}_2(\mu_4\text{-}C_2O_4)]^{2-}$, $[UO_2(NO_3)_3]^-$, and $[UO_2(NO_3)_4]^{2-}$. *Inorg. Chem.* **2004**, *43*, 2503–2514.

AR700068X